Arch. Metall. Mater. **63** (2018), 4, 1903-1908

DOI: 10.24425/amm.2018.125122

M. NOWAK*, Z. NOWAK*#, R.B. PĘCHERSKI*, M. POTOCZEK**, R.E. ŚLIWA**

ASSESSMENT OF FAILURE STRENGTH OF REAL ALUMINA FOAMS WITH USE OF THE PERIODIC STRUCTURE MODEL

The subject of the study are alumina foams produced by gelcasting method. The results of micro-computed tomography of the foam samples are used to create the numerical model reconstructing the real structure of the foam skeleton as well as the simplified periodic open-cell structure models. The aim of the paper is to present a new idea of the energy-based assessment of failure strength under uniaxial compression of real alumina foams of various porosity with use of the periodic structure model of the same porosity. Considering two kinds of cellular structures: the periodic one, for instance of *fcc* type, and the random structure of real alumina foam it is possible to justify the hypothesis, computationally and experimentally, that the same elastic energy density cumulated in the both structures of the same porosity allows to determine the close values of fracture strength under compression. Application of finite element computations for the analysis of deformation and failure processes in real ceramic foams is time consuming. Therefore, the use of simplified periodic cell structure models for the assessment of elastic moduli and failure strength appears very attractive from the point of view of practical applications.

Keywords: periodic cell structure, alumina open-cell foam, Young modulus, strength of alumina foams, Burzyński limit criterion

1. Introduction

Cellular materials such as open-cell alumina foams consist of spatial, three dimensional porous structure of randomly distributed interconnected pores. As already mentioned by Gibson and Ashby [1], morphology in relation with the mechanical properties of cellular materials is a challenging research area. A lot of research has been done during last years with focus on the experimental and numerical characterisation of the foam structure and its connection to the mechanical properties. Many papers have been devoted to describe the complex geometrical features of open-cell foams and the strength of such structures. Gibson and Ashby [1] reviewed the available correlations for prediction of the strength and investigated the behaviour of the wide range of different foams. Various open-cell foam models can be found in the literature. The most often used method to generate the foam structure is the Voronoi tessellation, [1], since it satisfies the topological requirement on edge and face connectivity. Jang et al. [2] studied models, which are based on Surface Evolver simulations of random soap froth with cells in spatially periodic domains. Roberts and Garboczi [3] analysed Voronoi tessellation and different stochastic approaches, such as sphere overlapping, Gaussian random fields and it appeared that the Voronoi tessellation shows a microstructure similar to the open-cell foam geometry. In Lu et al. [4], the actual random foam microstructures were approximated by regular structures of an elementary cells, cf. also Janus-Michalska and Pęcherski [5]. If the FEM is used for the calculation of the stress fields in the representative volume element (RVE) of the foam material, the region occupied by the skeleton should be discretized by finite element method. As a result, the number of the finite elements and computational cost of the problem increases essentially in comparison with the situation when the approximate solutions of the mechanical problems were obtained on the basis of the analysis of the regular elementary cell structures.

In this work, an attempt is made to estimate the strength of a realistic open-cell foam structure. It is possible to show that the periodic cell structure can be used to reproduce the realistic skeleton geometry by considering the mean values of window radius, variable cell radius and wall thickness distributions, (Nowak et al. [6,7]). The periodic foam structure is possible to generate by specification of the shape of elemental cell. This observation leads to the hypothesis that the numerical simulation of the deformation process under compression until failure performed for the periodic structure of *fcc* type, see Fig. 4, can provide an estimation of the failure strength of real alumina foams considered in the paper. The advantage of such an approach lies in its low computational cost, (Nowak et al. [8]). The main goal of the presented study is to provide theoretical background supporting the above mentioned hypothesis. The energy-based theory of material effort, material strength, in relation to materials revealing the strength differential effect (SDE)

* INSTITUTE OF FUNDAMENTAL TECHNOLOGICAL RESEARCH, POLISH ACADEMY OF SCIENCES, PAWIŃSKIEGO 5B, 02-106 WARSAW, POLAND
** RZESZÓW UNIVERSITY OF TECHNOLOGY, POWSTAŃCÓW WARSZAWY 12, 35-959 RZESZÓW, POLAND
# Corresponding author: znowak@ippt.pan.pl

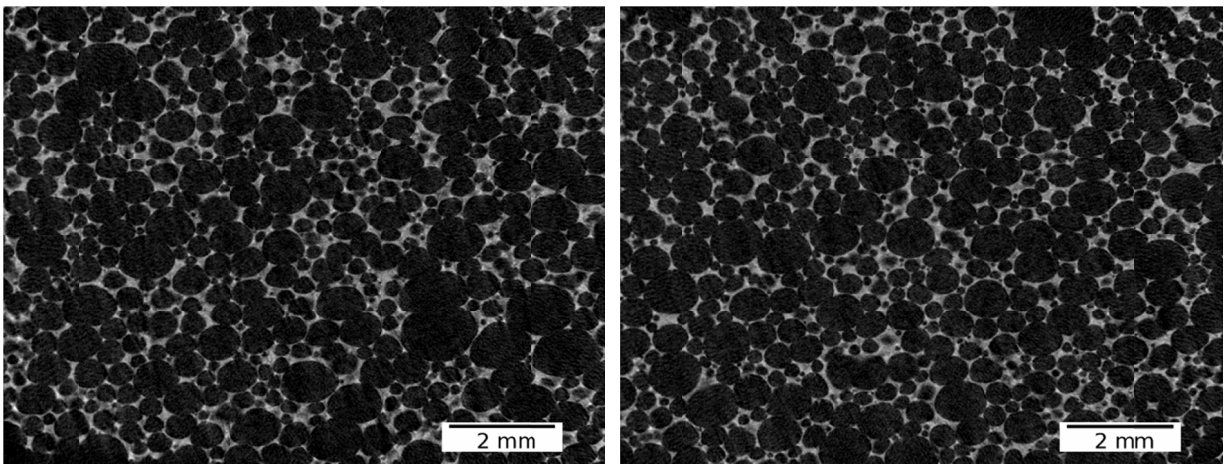

Fig. 1. Example of typical cross-sections images of the alumina foam sample with porosity of 86%

was developed originally by Burzyński [9,10], cf. e.g. Vadillo et al. [11] in application to metal plasticity. In particular within the context of ceramic foams the energy-based theory leads to an ellipsoidal limit elastic condition, Pęcherski et al. [12], Zhang et al. [13]. The proposed method of assessment of failure strength of real alumina foam is compared and validated with analytical Gibson method and experimental data.

2. Computed microtomography observations

The computed tomography technique is used to reconstruct the real geometry of alumina foam. Experimental studies of sample foam with 86% are carried out using the X-Ray Microtomograph SkyScan 1174. The typical cross-sections images obtained from the studies are shown in Fig. 1. The size of the individual pixel is equal 2.54 μm and the image size is 1535 × 1164 pixels. This image resolution gives the detail structure of the foam without neglecting its relevant characteristics.

The obtained sequence of digital images are used for further processing with application of ScanIP software [14]. The 3D model of the foam structure is created by applying the

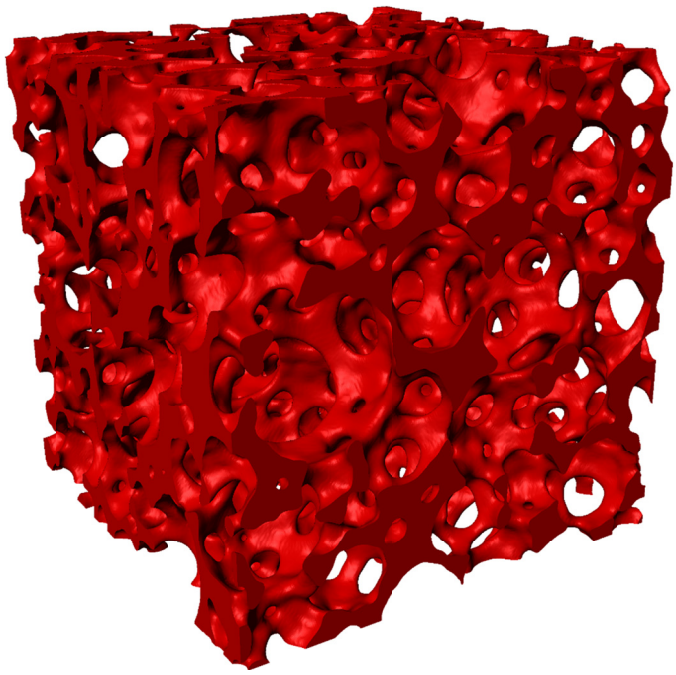

Fig. 2. The three-dimensional numerical model of real alumina foam generated using ScanIP software [14]

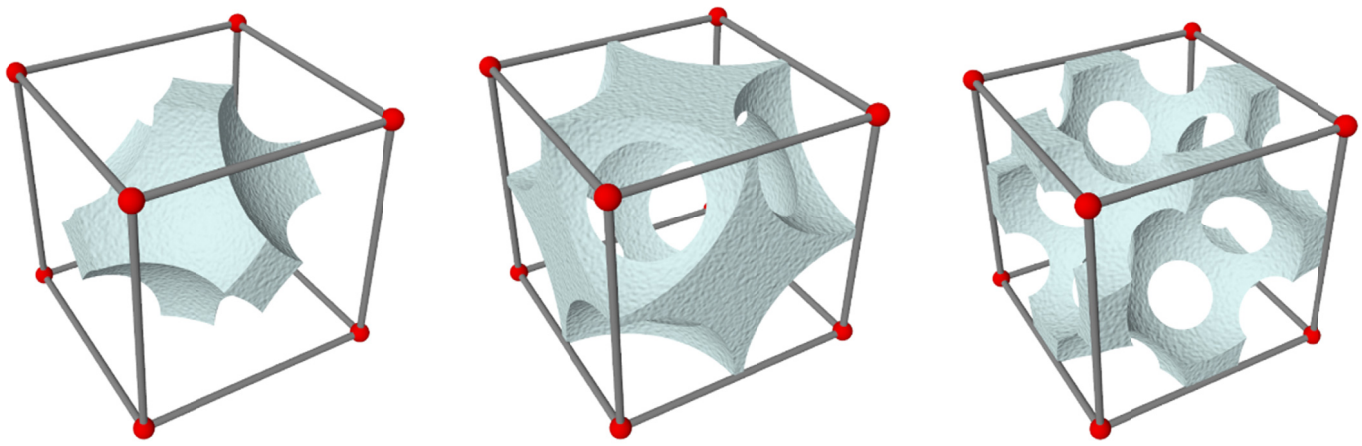

a) b) c)

Fig. 3. Periodic cell models a) *sc*, b) *bcc*, c) *fcc*

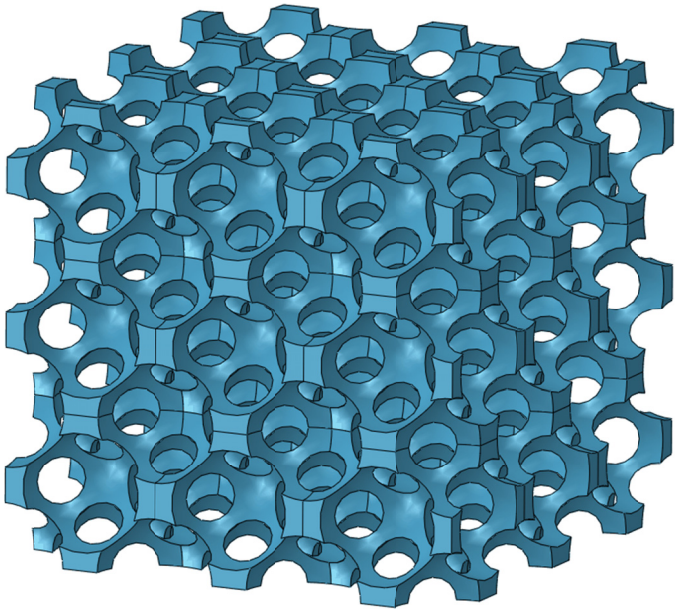

Fig. 4. Periodic foam structure based on *fcc* unit cell

threshold value and Gaussian filtering. The detailed description of the model generation is presented by authors in Nowak et al. [8]. The final result of digital processing of images is shown in Fig. 2.

The obtained model of the foam has complex structure. It is possible to develop simplified equivalent model of periodic cell structure with the same porosity. The parameters describing the foam structure are determined on the basis of the computed microtomography observations. It can be assumed that those parameters are the mean values of window radius, cell radius and wall thickness distributions. They can be calculated with use of developed numerical procedure described in Nowak et al. [8].

3. Periodic cell models

The distributions of the window radius and the wall thickness in the real alumina ceramic foams make the basis for the generation of the particular periodic cell models. The foam structures: simple cubic (*sc*), body centered cubic (*bcc*) and face centered cubic (*fcc*) represented by the shape of one cell are presented in Fig. 3.

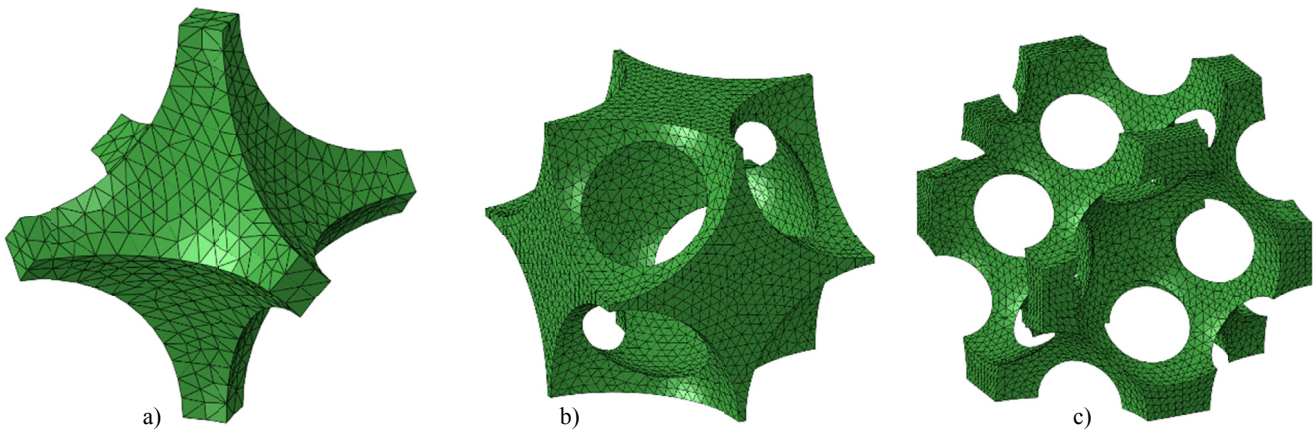

Fig. 5. Finite element mesh for periodic cell models a) *sc*, b) *bcc*, c) *fcc*

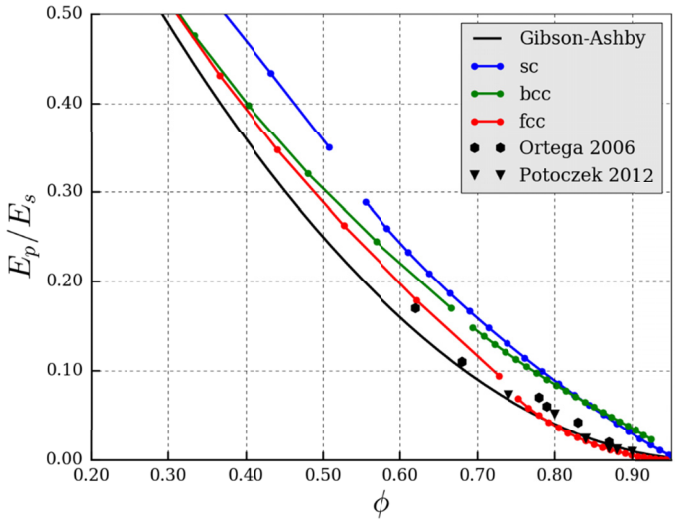

Fig. 6. The relative Young modulus as a function of porosity for three types of periodic cell models *sc*, *bcc*, *fcc* confronted with experimental data, E_p and E_s denote the Young modulus for porous (cellular) and solid material, respectively

The unit cell of *fcc* type is replicated in three directions. The periodic *fcc* structure is presented in Fig. 4.

The numerical simulations of compression processes of the samples with three periodic cell models of finite element mesh shown in Fig. 5 leads to the conclusion that the *fcc* structure provides the best estimation of experimental results depicted in Fig. 6.

4. Material model of solid alumina

One of the most important aspects in numerical simulation of the material deformation is to formulate constitutive material model. In this work two constitutive models of solid alumina are used. The elastic part of deformation for solid alumina describes

isotropic Hooke's law

$$\boldsymbol{\sigma} = 2G_S\boldsymbol{\varepsilon} + \lambda_S tr(\boldsymbol{\varepsilon}) \tag{1}$$

where $G_S = E_S/2(1+\nu)$, and Lame parameter is equal $\lambda_S = E_S\nu/(1+\nu)(1-2\nu)$. E_S defines Young modulus and ν is the Poisson ratio for solid material.

In terms of small deformations and when the stress level is much smaller than the elastic limit, the Hooke's model is a good way to describe the behaviour of solid alumina. For this range of deformation there is no damage caused by brittle cracking. Therefore, this model is used to determine the Young modulus E_p of the foam based on numerical simulation of compression test.

The elastic limit surface of solid alumina is described by Burzyński criterion (Burzyński [9,10], Pęcherski et al. [12]). According to the original proposition of W. Burzyński the limit condition in terms of elastic energy density is proposed as the hypothesis of variable limit energy of volume change and distortion:

$$\Phi_f + \eta(p)\Phi_v = K$$
$$\eta = \omega + \frac{\delta}{3p}, \qquad p = \frac{\sigma_1+\sigma_2+\sigma_3}{3} \tag{2}$$

where Φ_f – density of elastic energy of distortion and Φ_v – density of elastic energy of volume change.

The following replacement of material constants $(\omega, \delta, K) \rightarrow (\sigma_Y^T, \sigma_Y^C, \tau_Y)$ allows to express the criterion (2) in terms of the limit stress in tension σ_Y^T, compression σ_Y^C and shear τ_Y.

$$\frac{\sigma_Y^T\sigma_Y^C}{6\tau_Y^2}\left[(\sigma_1-\sigma_2)^2+(\sigma_2-\sigma_3)^2+(\sigma_3-\sigma_1)^2\right]+$$
$$+\left(1-\frac{\sigma_Y^T\sigma_Y^C}{3\tau_Y^2}\right)(\sigma_1+\sigma_2+\sigma_3)^2+$$
$$+(\sigma_Y^C-\sigma_Y^T)(\sigma_1+\sigma_2+\sigma_3) - \sigma_Y^C\sigma_Y^T = 0 \tag{3}$$

In this way the known quadric equation is obtained. The interplay of material constants $(\sigma_Y^T, \sigma_Y^C, \tau_Y)$ leads to different limit surfaces of the second order: parabolid, ellipsoid, cone or cylinder, Burzyński [9], Vadillo et al. [11] and Pęcherski et al. [12].

In case of solid alumina the paraboloid limit elastic surface is suitable:

$$F = q^2 + 3\left(\sigma_Y^C - \sigma_Y^T\right)p - \sigma_Y^C\sigma_Y^T = 0 \tag{4}$$

where the symbol $q = \sqrt{3/2\,\boldsymbol{s}:\boldsymbol{s}}$ defines the equivalent stress and $\boldsymbol{s}$ is the deviatoric stress tensor while p is the hydrostatic pressure. It can be shown that for porous and in particular cellular materials the ellipsoid limit elastic surface can be applied.

In the space of principal stresses $(\sigma_1, \sigma_2, \sigma_3)$ Eq. 4 defines the axisymmetric paraboloid around the hydrostatic axis (Fig. 7).

The points inside the paraboloid define the stress states for which material behaves elastically. Reaching the limit surface is associated with the initiation of damage. To describe the inelastic behaviour the additive decomposition of strain tensor is used

$$\dot{\boldsymbol{\varepsilon}} = \dot{\boldsymbol{\varepsilon}}^e + \dot{\boldsymbol{\varepsilon}}^{in} \tag{5}$$

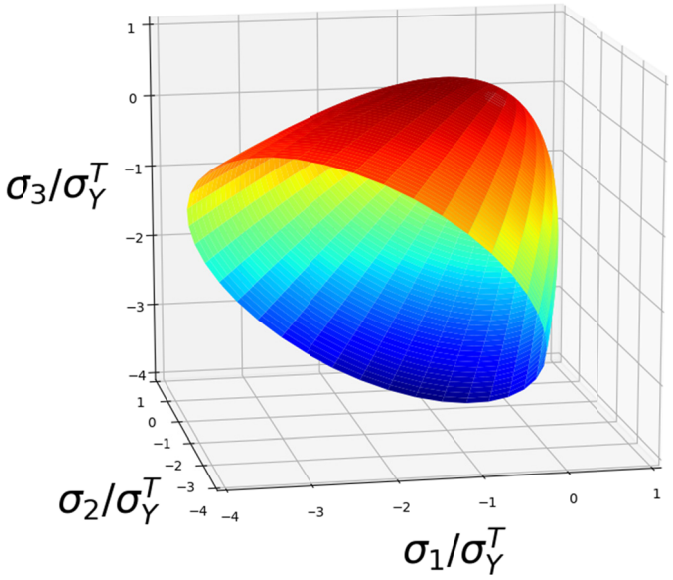

Fig. 7. The limit surface for solid alumina for parameters $\sigma_Y^C = 2400$ MPa and $\sigma_Y^C = 105$ MPa

The constitutive model for inelastic part of deformation is described by associated flow rule

$$\dot{\boldsymbol{\varepsilon}}^{in} = \dot{\lambda}\frac{\partial G}{\partial \boldsymbol{\sigma}}, \text{ where } G = F \tag{6}$$

and $\dot{\lambda}$ is the unknown multiplier. The scalar damage parameter d (Kachanov [15]) is adopted into stress-strain relation. This gives the following formula (Lubliner [16])

$$\boldsymbol{\sigma} = (1-d)\,\boldsymbol{D}^e : (\boldsymbol{\varepsilon} - \boldsymbol{\varepsilon}^{in}) \tag{7}$$

where $d = 0$ corresponds to no damage and $d = 1$ is the total failure. The scalar damage parameter is proposed to be a function η of equivalent strain $\bar{\varepsilon}^{in}$ in the form

$$d = \eta(\bar{\varepsilon}^{in}) \tag{8}$$

where the equivalent strain is calculated from the equation (Lubliner [16])

$$\boldsymbol{\sigma} : \dot{\boldsymbol{\varepsilon}}^{in} = \sigma_Y^C\,\dot{\bar{\varepsilon}}^{in} \tag{9}$$

The aforementioned constitutive model has been implemented in UMAT subroutine for ABAQUS finite element program [17]. This model is used to determine the compressive strength of the alumina foam.

5. Numerical simulation of the periodic structure compression

Numerical simulations of the uniaxial compression of the periodic *fcc* structure outlined in Section 3 to predict the compressive strength of alumina foams is conducted with use of ABAQUS finite element program. The ceramic foam is assumed

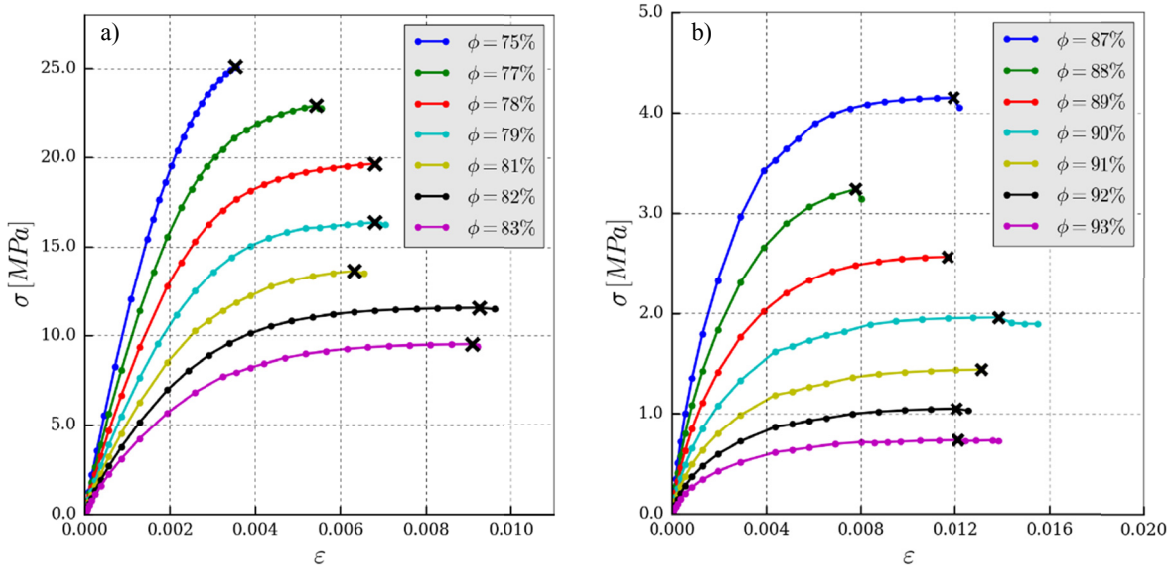

Fig. 8a) and b). The stress-strain curves obtained in numerical simulations of the compression test of *fcc* periodic cell model with different values of porosity

to be isotropic. The bottom surface of the sample is fixed and the top surface of the sample moves parallel to the z-axis. The following material model is assumed: Young modulus $E_0 = 370$ GPa and Poisson's ratio $\nu = 0.22$. In the calculations the function η is assumed as the linear function of $\overline{\varepsilon}^{in}$ with the limits of the initial value, $\eta(0) = 0$, and final value for $\overline{\varepsilon}^{in} = \overline{\varepsilon}_c^{in}$, $\eta(\overline{\varepsilon}_c^{in}) = 0.9$.

The results of numerical simulations of compression test of the foam specimens with different values of porosity are presented in Fig. 8. The marked limit points on the stress-strain curves correspond to the maximum value of calculated compression stress and are considered as the failure stress points.

The values of failure strength σ_f^C calculated for different porosities are compared with the experimental data obtained by Nowak [18] and Potoczek [19], Fig. 9. Also the results of analytical model presented by Gibson and Ashby [1] is confronted.

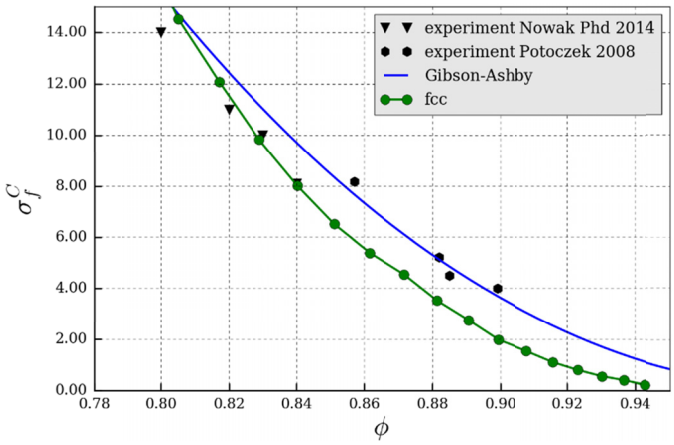

Fig. 9. Comparison of computed failure strength σ_f^C with experimental data and analytical model of Gibson and Ashby [1] as a function of porosity

6. The energy-based equivalence hypothesis

Considering two kinds of cellular structures: the periodic one, e.g. of *fcc* type, and the random one corresponding to real alumina foam one can state the hypothesis that the same elastic energy density cumulated in the both structures determines the same values of fracture strength σ_f^C under compression. This energy-based equivalence hypothesis can be validated under the assumption that, the limit states of linear elasticity of the alumina skeleton are considered.

The limit condition (3) for the case of uniaxial compression $\sigma_3 = -\sigma$, $\sigma_1 = \sigma_2 = 0$ leads to:

$$\sigma = \sigma_Y^C \tag{10}$$

This means that for ceramics under uniaxial compression the equivalence of the elastic energy density $\Phi = \frac{1}{2}\frac{\sigma^2}{E}$:

$$\Phi_{fcc} = \Phi_{real} \tag{11}$$

leads to the following assessment of the failure strength of real foam under compression:

$$\left(\sigma_f^C\right)_{real} = \left(\sigma_f^C\right)_{fcc}\sqrt{\frac{E_{real}}{E_{fcc}}} \tag{12}$$

In Fig. 10 the comparison of the failure strength $\left(\sigma_f^C\right)_{fcc}$ with the estimated strength $\left(\sigma_f^C\right)_{real}$ is presented.

7. Summary and conclusions

The microstructure of alumina open-cell foams is characterized using computed X-ray microtomography. As a result the numerical model reconstructing the real foam structure and the simplified periodic open-cell structure models are obtained. It appears that the *fcc* structure provides the best estimation of experimental data shown in Fig. 6. The performance of the

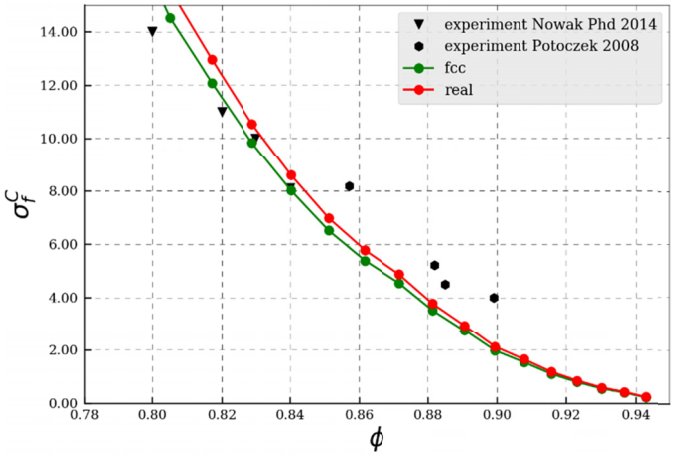

Fig. 10. The comparison of the failure strength $(\sigma_f^C)_{fcc}$ with the estimated strength $(\sigma_f^C)_{real}$ and experimental data as a function of porosity

both reconstructed models is compared with measured values of the elastic moduli and strength under uniaxial compression. The following observations can be made from this comparison:

- prediction of Young's moduli obtained from the reconstructed models of real and *fcc* type structures are in agreement with the measured values,
- prediction of the strength values under compression of the generated *fcc* type skeleton are close to the values obtained in the finite element computations made for the reconstructed real foam structure, cf. Fig. 10,
- the energy-based equivalence hypothesis can be extended to foams and cellular materials of metallic skeleton, at least for the case of elastic limit strength.

Acknowledgements

Financial support of Structural Funds in the Operational Program Innovative Economy (IE OP) financed from the European Regional Development Fund Project "Modern material technologies in aerospace industry", Nr POIG.01.01.02-00-015/08-00 is gratefully acknowledged.

REFERENCES

[1] L.J. Gibson, M.F. Ashby, Cellular Solids, Structure and Properties, 2nd edition, Cambridge (1999).

[2] W.-Y. Jang, A.M. Kraynik, S. Kyriakides, On the microstructure of open-cell foams and its effect on elastic properties, Int. J. Solids and Struct. **45** (7), 1845-1875 (2008).

[3] A.P. Roberts, E.J. Garboczi, Elastic properties of model random three-dimensional open-cell solid, J. Mech. Phys. Solids **50**, 33-55 (2002).

[4] T. Lu, H. Stone, M. Ashby, Heat transfer in open-cell metal foams Acta Mater. **46**, 3619 -3635 (1998).

[5] M. Janus-Michalska, R.B. Pęcherski, Macroscopic properties of open-cell foams based on micromechanical modelling, Technische Mechanik **23**, 234-244 (2003).

[6] M. Nowak, Z. Nowak, R.B. Pęcherski, M. Potoczek, R.E. Śliwa, On the reconstruction method of ceramic foam structures and the methodology of Young modulus determination, Archives of Metallurgy and Materials **58**, 1219-1222 (2013).

[7] Z. Nowak, M. Nowak, R.B. Pęcherski, M. Potoczek, R.E. Śliwa, Mechanical properties of the ceramic open-cell foams of variable cel sizes, Archives of Metallurgy and Materials **60**, 1957-1963 (2015).

[8] Z. Nowak, M. Nowak, R. Pęcherski, M. Potoczek, R.E. Śliwa, Numerical simulations of mechanical properties of alumina foams based on computed tomography, Journal of Mechanics of Materials and Structures **1**, 107-121 (2017).

[9] W. Burzyński, Selected passages from Włodzimierz Burzyński doctoral dissertation Study on Material Effort Hypotheses, Engineering Transactions **57**, 185-215 (2009).

[10] W. Burzyński, Über die Anstrengungshypothesen. Schweizerische Bauzeitung **94** (21), 259-262 (1929).

[11] G. Vadillo, J. Fernandez-Saez, R.B. Pęcherski, Some applications of Burzynski yield condition in metal plasticity, Materials and Design **32**, 628-635 (2011).

[12] R.B. Pęcherski, K. Nalepka, T. Fraś, M. Nowak, Inelastic Flow and Failure of Metallic Solids. Material Effort: Study Across Scales, in : Constitutive Relations under Impact Loadings. Experiments, Theoretical and Numerical Aspects, Łodygowski T., Rusinek A. (eds.), Springer, CISM, Udine **552**, 245-285 (2014).

[13] S. Zhang, M. Guan, G. Wu, S. Gao, X. Chen, An ellipsoidal yield criterion for porous metals with accurate descriptions of theoretical strength and Poisson's ratio, Acta Mechanica **228**, 4199-4210 (2017).

[14] ScanIP, ver. 7.0 (2014), http://www.simpleware.com/software/scanip.

[15] L.M. Kachanov, On time to failure in creep conditions, Izv. Ak. Nauk SSSR OTN, **8**, pp. 26-31 (1958).

[16] J. Lubliner, J. Oliver, S. Oller, E. Oñate, A plastic-damage model for concrete, International Journal of Solids and Structures **25**, 299-326 (1989).

[17] Simulia, ABAQUS/Standard User's Manual, Version 6.13 Edition. Dassault Systemes, Providence, USA (2013).

[18] M. Nowak, Analysis of deformation and failure of ceramic foam structures in application to numerical simulation of infiltration processes of alumina foam by liquid metal, PhD thesis, in Polish, IPPT PAN, Warsaw (2014).

[19] M. Potoczek, Gelcasting of alumina foams using agarose solutions, Ceramics International **34**, 661-667 (2008).